2011-11

Supramolecular architectures in layer-by-layer films of single-walled carbon nanotubes, chitosan and cobalt (II) phthalocyanine

Materials Chemistry and Physics, Lausanne : Elsevier, v. 130, n. 3, p. 1072-1077, Nov. 2011
http://www.producao.usp.br/handle/BDPI/50083

Materials Chemistry and Physics 130 (2011) 1072–1077

Contents lists available at SciVerse ScienceDirect

Materials Chemistry and Physics

journal homepage: www.elsevier.com/locate/matchemphys

Supramolecular architectures in layer-by-layer films of single-walled carbon nanotubes, chitosan and cobalt (II) phthalocyanine

Roberto A. de Sousa Luz[a], Marccus Victor A. Martins[a], Janildo L. Magalhães[a], José R. Siqueira Jr.[b], Valtencir Zucolotto[c], Osvaldo N. Oliveira Jr.[c], Frank N. Crespilho[d], Welter Cantanhêde da Silva[a,*]

[a] Departamento de Química, Centro de Ciências da Natureza, Universidade Federal do Piauí, Teresina – PI, CEP 64049-550, Brazil
[b] Instituto de Ciências Exatas, Naturais e Educação, Universidade Federal do Triângulo Mineiro, Uberaba – MG, CEP 38025-180, Brazil\
[c] Instituto de Física de São Carlos, Universidade de São Paulo, São Carlos – SP, CEP 13560-970, Brazil
[d] Centro de Ciências Naturais e Humanas, Universidade Federal do ABC, Santo André – SP, CEP 09210-170, Brazil

ARTICLE INFO

Article history:
Received 4 February 2011
Received in revised form 21 July 2011
Accepted 21 August 2011

Keywords:
Thin films
Multilayers
Nanostructures, Electrochemical techniques

ABSTRACT

The building of supramolecular structures in nanostructured films has been exploited for a number of applications, with the film properties being controlled at the molecular level. In this study, we report on the layer-by-layer (LbL) films combining cobalt (II) tetrasulfonated phthalocyanine (CoTsPc), chitosan (Chit) and single-walled carbon nanotubes (SWCNTs) in two architectures, $\{Chit/CoTsPc\}_n$ and $\{Chit\text{-}SWCNTs/CoTsPc\}_n$ ($n = 1$–10). The physicochemical properties of the films were evaluated and the multilayer formation was monitored with microgravimetry measurements using a quartz microbalance crystal and an electrochemical technique. According to atomic force microscopy (AFM) results, the incorporation of SWCNTs caused the films to be thicker, with a thickness ca. 3 fold that of a 2-bilayer LbL film with no SWCNTs. Cyclic voltammetry revealed a quasi-reversible, one electron process with $E_{1/2}$ at −0.65 V (*vs* SCE) and an irreversible oxidation process at 0.80 V in a physiological medium for both systems, which can be attributed to $[CoTsPc(I)]^{5-}/[CoTsPc(II)]^{4-}$ and CoTsPc(II) to CoTsPc(III), respectively. The $\{Chit\text{-}SWCNTs/CoTsPc\}_5$ multilayer film exhibited an increased faradaic current, probably associated with the supramolecular charge transfer interaction between cobalt phthalocyanine and SWCNTs. The results demonstrate that an intimate contact at the supramolecular level between functional SWCNTs immobilized into biocompatible chitosan polymer and CoTsPc improves the electron flow from CoTsPc redox sites to the electrode surface.

1. Introduction

Supramolecular chemistry has been conceived as the chemistry governed by association of two or more species interacting non-covalently to produce highly complex structures [1,2]. Concepts from supramolecular and molecular chemistry have been linked by Lehn [3] in the so-called constitutional dynamic chemistry (CDC), which is relevant for such dynamic aspects as reversible bonds, self-organization, molecular recognition, and donor–acceptor interactions [3]. CDC is promising for nanoscience and nanotechnology, for new properties and reactivity from functional supramolecular architectures can be obtained and interpreted [4]. For the fabrication of controlled architectures, the Langmuir–Blodgett (LB) and the Layer-by-Layer (LbL) techniques [5] are among the most used, with which nanomaterials can be produced with distinctive electronic, optical, electrochemical and catalytic properties. The LbL technique [6] was initially based on adsorbing oppositely charged polyelectrolytes from solution, and variations now include spin-assisted LbL [7] and spray based LbL [8] depositions. It has been used to immobilize organic and inorganic nanomaterials [9], carbon nanotubes [10], metallophthalocyanines [11–13], conducting polymers [7,14], metallic nanoparticles [11,15], enzymes [10], DNA [16] and antigen–antibody pairs [17]. Interestingly, supramolecular effects arise in these films owing to the close contact between the layers of materials deposited [1–3]. Unique properties of LbL films can now be exploited in sensors [18,19], biosensors [16], and optical devices [20,21].

In a recent work, we used the CDC concepts to control chemical properties of metallophthalocyanines in LbL films [11] exploring the sensing activity in these platforms. The CDC effects were initially apparent [11] through charge transfer interaction between gold nanoparticles (AuNPs) and nickel phthalocyanines in 3-bilayer LbL films, with the architecture ITO-$\{PAH\text{-}AuNPs/NiTsPc\}_3$ (PAH = poly-allylamine hydrochloride). This system exhibited an electrocatalytic oxidation for hydrogen peroxide, increasing the faradaic currents of the redox processes attributed to the

* Corresponding author. Tel.: +55 086 3215 5840; fax: +55 086 3215 5692.
E-mail address: welter@ufpi.edu.br (W.C. da Silva).

0254-0584/$ – see front matter © 2011 Elsevier B.V. All rights reserved.
doi:10.1016/j.matchemphys.2011.08.038

phthalocyanine ligand and Ni^{2+}/Ni^{3+} couple. A different behavior was observed for an ITO-{PAH/NiTsPc}$_3$ electrode (without AuNPs), where only the TsPc ligand process was affected [11]. In another study, the supramolecular organization of cobalt (II) phthalocyanine in nanostructured films had a remarkable influence on the final redox properties of the PAH/FtTsCo system. The latter were more sensitive electrodes than those with the PAH/FtTsNi and PAH-AuNPs/FtTsNi systems, in addition to displaying a high catalytic performance for the oxidation of cysteine [13].

With the CDC effects observed owing to gold nanoparticles, one could wonder whether the same would apply to other types of nanomaterial, which have also been exploited to produce LbL films. Of particular interest are the carbon nanotubes (CNTs) [22] that may be single-walled (SWCNTs) or multi-walled (MWCNTs) and have structure-dependent properties [23,24]. Indeed, SWCNTs have rich electronic properties, high surface area, excellent mechanical strength and thermal stability [25]. Such characteristics are ideal to develop new nanoelectrochemical devices with elevated performance in sensors [24], biosensors [26], and free radical scavenging applications [27]. SWCNTs can also be combined with other substances, such as polymers [28] and metallic nanoparticles [15], leading to functional films [10,23,24]. With regard to finding suitable template materials to obtain LbL films, we have chosen chitosan (Chit), which is a biodegradable natural cationic polysaccharide with excellent biocompatibility and low toxicity, used as anti-bacterial agent, drug delivery system and for immobilizing enzymes [29,30]. In this study, chitosan was employed as polymeric matrix to disperse SWCNTs, which were then combined with cobalt (II) phthalocyanine to form supramolecular architectures. The LbL technique was the strategy to combine the advantageous features of SWCNTs, chitosan and cobalt (II) phthalocyanines. The main aim was to investigate the supramolecular charge transfer between CoTsPc and SWCNTs in the multilayers, which will be useful for creating new platforms with bioactivity, high electrochemical stability and good selectivity for sensing.

2. Experimental

Cobalt(II) tetrasulfonated phthalocyanine (CoTsPc) was purchased from Porphyrin Systems and used without further purification. Carboxylic acid functionalized single-walled carbon nanotubes (SWCNTs-COOH) were obtained from Aldrich. These nanotubes were produced with the arc discharge technique and purified with nitric acid (purity of 80–90%), having a length of 0.5–1.5 μm and diameter of 1.5 nm and 3–5 nm for individual and bundled samples, respectively. Chitosan (Chit) was acquired from Polymar Science and Nutrition company (Ceará, Brazil). Acetic acid (CH_3COOH), purchased from Reagen, with concentration of 1% (pH 4.0) was used as solvent for preparing electrolytic solutions. Dihydrogen sodium phosphate (NaH_2PO_4), monohydrogen sodium phosphate (Na_2HPO_4) and sodium chloride (NaCl), also from Reagen, were used to prepare the supporting electrolyte 0.1 mol L^{-1} (pH 6.8) NaH_2PO_4/Na_2HPO_4 – (PBS – phosphate buffer solution). All aqueous solutions were obtained with water supplied by a Millipore system (Milli-Q). CoTsPc and Chitosan solutions had a concentration of ~0.5 g L^{-1} in 1% acetic acid (pH 4.0). The nanobiocomposite (Chit-SWCNTs) was prepared by dissolving 1.0 mg of SWCNTs in 10 mL of chitosan 0.5 g L^{-1} at pH 4.0 through sonication for 1 h, and used as cationic polyelectrolyte.

The nanostructured films were produced with the LbL method [6], using hydrophilic glass or previously cleaned [31] indium tin oxide (ITO) substrates. The substrate, with a negatively charged surface, was immersed into a biopolymer solution (Chit-SWCNTs or Chit) for 5 min, rinsed with pH 4.0 acetic acid solution to remove the excess of material and then dried under a nitrogen stream (99.9% purity). A layer was formed owing to electrostatic interaction between the substrate and the polyelectrolyte solution. In a second step, the substrate was immersed into the solution of the negatively charged CoTsPc for 5 min, followed again by rinsing with pH 4.0 acetic acid solution and drying steps, to form the first bilayer. This process was repeated until the desired number of bilayers was obtained. Fig. 1 illustrates a schematic representation of the LbL assembly {Chit-SWCNTs/CoTsPc}$_n$, where n represents the number of bilayers.

The UV–Vis spectra of CoTsPc and Chit-SWCNTs solutions and the {Chit/CoTsPc}$_n$ and {Chit-SWCNTs/CoTsPc}$_n$ LbL films, on hydrophilic glass substrates, were measured with a Hitachi U-3000 spectrophotometer. The multilayer growth for both architectures was monitored using quartz crystal microbalance (QCM, 200 – SRS) measurements, with a gold foil as substrate. The film morphology was investigated in Chit/CoTsPc and Chit-SWCNTs/CoTsPc films containing 1, 2 and 5 bilayers deposited onto ITO using an atomic force microscope (AFM) Nanoscope III from Digital Instruments. The electrochemical experiments were carried out with a potentiostat Autolab Eco Chemie PGSTAT 30, employing a conventional three-electrode cell at room temperature (~25 °C). Voltammetric measurements were performed with a saturated calomel electrode (SCE) and platinum (area = 0.65 cm^2) as reference and auxiliary electrodes, respectively, while the modified ITO (area = 0.35 cm^2) with {Chit/CoTsPc}$_n$ or {Chit-SWCNTs/CoTsPc}$_n$ LbL films was used as the working electrode. Various scan rates were used for both film architectures, so that the influence of the number of bilayers (n) on the modified electrode could be studied. Before each measurement the oxygen dissolved in the electrolytic solution was removed with a nitrogen flow during 10 min.

3. Results and discussion

3.1. UV-Visible and FTIR spectroscopy: supramolecular organization of multilayer films

The absorption bands in the UV–Vis spectra are normally employed to monitor LbL film growth for MTsPc and CNTs, as the absorption intensity may be taken as proportional to the amount of adsorbed CoTsPc and Chit-SWCNTs [11–13]. However, the Chit-SWCNTs band may have a molar extinction coefficient much lower than for the Q band of CoTsPc, and therefore it was not used to monitor growth of the SWCNTs layers. Fig. S1 in the Supplementary Information shows the UV–Vis spectra for Chit, Chit-SWCNTs (a), and CoTsPc (b) solutions, as well as for 5-bilayer LbL films of Chit-SWCNTs/CoTsPc and Chit/CoTsPc (b). The Chit-SWCNTs nanocomposite exhibited a band at 215 nm, characteristic of carbon nanotubes dispersed in solution as shown in Fig. S1 [32]. On the other hand, the chitosan solution did not show electronic transitions in the range from 190 to 800 nm. The {Chit-SWCNTs/CoTsPc}$_n$ and {Chit/CoTsPc}$_n$ systems exhibited a Soret band at 338 nm and an intense Q band between 550 and 700 nm, assigned to the porphyrin rings (FtTs ligand) and CoTsPc species (Fig. S1). This latter band may comprise high and low energy transitions attributed to the monomer and dimeric species, respectively [9,11–13]. For 5-bilayer LbL films of Chit/CoTsPc and Chit-SWCNTs/CoTsPc, bands at 616 and 618 were observed (Fig. S1), which are assigned to dimeric species. In addition, a shoulder at 672 nm due to the monomer transition was noted, in agreement with the literature for several LbL films [12,13,33]. A similar behavior for CoTsPc was observed in {Chit/CoTsPc}$_n$ and {PAH/CoTsPc}$_n$ systems, suggesting that a change in the building block in hybrid nanoarchitectures does not alter the geometry and/or electronic configuration of the CoTsPc complex [11–13].

The level of supramolecular organization of CoTsPc in LbL films with poly-(allylamine hydrochloride) (PAH) was evaluated based on the relative importance of dimer and monomer species in the films, as indicated by the ratio between the absorption intensities (I_{dim}/I_{mon}) [13]. Upon analyzing the absorption spectra, a large amount of H-aggregates with dimers was found for PAH/CoTsPc LbL films with 5 through 20 bilayers [13]. In this study, {Chit/CoTsPc}$_n$ LbL films with up to 10 bilayers had I_{618}/I_{672} of 1.75 for 1-bilayer film, then reaching 1.84 for the 5-bilayer LbL film. Significantly, after SWCNTs immobilization in the chitosan matrix the relative intensities (I_{618}/I_{672}) decreased to 1.16 for all multilayers, which is the same for CoTsPc species in solution ($I_{633}/I_{667} = 1.16$) (Supplementary Information, Table S1). This indicates that CoTsPc molecules in LbL films containing SWCNTs are organized in a more dispersed fashion, probably avoiding a π-stacking conformation [13]. This behavior can be explained by the supramolecular stabilization between $-SO_3^-$ (from CoTsPc) and $-NH_3^+$ (from chitosan) groups (Fig. 1), with a more uniform CoTsPc distribution across the film [13]. Fig. 2 depicts the LbL film growth, where the band intensity at 616 and 618 nm increased linearly up to 10 bilayers, indicating a uniform deposition for CoTsPc.

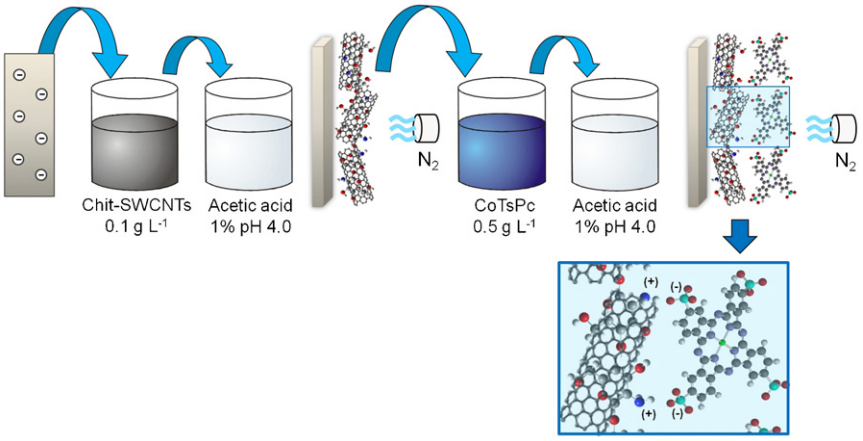

Fig. 1. Schematic representation of the LbL assembly method for 1-bilayer Chit-SWCNTs/CoTsPc film. Detail: electrostatic interaction between the protonated amine group of chitosan and the negative sulfonic group from FtTsCo.

The adsorption and the supramolecular interaction between Chit (or Chit-SWCNTs) and CoTsPc were investigated with transmission-mode FTIR spectroscopy. The spectra for Chit, Chit-SWCNTs and CoTsPc cast films and 40-bilayer Chit/CoTsPc and Chit-SWCNTs/CoTsPc LbL films on silicon substrates are shown in Fig. S2 in Supplementary Information. The spectra of Chit and Chit-SWCNTs featured a broad absorption from 1660 to 1000 cm^{-1}, assigned to N–H and C–H deformations and C–N stretching in chitosan. Additional low intensity bands for the cast Chit film appeared at 1376 and 1412 cm^{-1} attributed to the C–H angular deformations, in addition to the N–H angular deformations at 1592 and 1662 cm^{-1}. For cast Chit-SWCNTs film two strong bands at 1419 and 1594 cm^{-1} were observed, assigned to C=C and C=O (carboxylic groups) stretching, respectively [34]. The latter are associated with the intermolecular phonons from carbon nanotubes [11,34], confirming the SWCNTs incorporation into the chitosan matrix. This incorporation was also corroborated by TEM measurements, which show the coating of chitosan on the surface of carbon nanotubes (Fig. S3, Supplementary Data). For the NiTsPc spectrum two main vibrational bands (strong intensity) were found at 1031 and 1191 cm^{-1} assigned to the S–O symmetric stretching and S=O symmetric stretching, respectively. Vibrational modes of medium intensity appeared between 600 and 850 cm^{-1}, associated with stretching and deformation of the macrocyclic ring. The low intensity bands were assigned as follows: 1398 cm^{-1} (isoindole stretching), 1330 cm^{-1} (S=O asymmetric stretching), 1110 cm^{-1} (C–H angular deformation), and 1056 cm^{-1} (S–O symmetric stretching). For the LbL films, the bands included ν(N–H), δ(N–H), ν(S=O), ν(S–O) and from the macrocyclic ring, which have been reported for Chit, Chit-SWCNTs and CoTsPc [11,18]. Most importantly, the band at 1031 cm^{-1} in the CoTsPc spectrum was shifted to lower energies in the spectra for the LbL films, thus suggesting the salt-bridge formation through supramolecular interaction between NH_3^+ and SO_3^- groups from Chit (or Chit-SWCNTs) and CoTsPc, respectively. These findings are similar to those in the literature for LbL films containing MTsPc (M = Fe, Ni or Cu), AuNPs and MWCNTs [11,18].

3.2. Growth and immobilization of Chit-SWCNTs/CoTsPc and Chit/CoTsPc multilayer films studied with QCM and AFM

The growth of Chit/CoTsPc and Chit-SWCNTs/CoTsPc LbL multilayers was monitored by measuring the change in frequency in a quartz crystal balance. Fig. 3 shows the increase in mass due to the deposition of Chit (or Chit-SWCNTs) and CoTsPc layers on the crystal, which was similar for both systems up to 7 bilayers. For thicker LbL films a small difference in mass change occurred, which may indicate that the incorporation of single-wall carbon nanotubes in the chitosan matrix induces strong stabilization of multilayer deposition with a smaller change in frequency.

The film morphology as studied with AFM [35] was globular for the first layer of Chit, Chit-SWCNTs and CoTsPc films, as indicated in Fig. 4. Upon increasing the number of bilayers, the thickness and roughness increased as expected. Though films with only 3 numbers of bilayers were deposited, it is already possible to observe that the thickness does not increase linearly with the number of bilayers (Supplementary Information, Table S2), which may be ascribed to interpenetration of adjacent layers. Such interpenetration occurs even for traditional polyelectrolytes [36], and would only to be expected especially for the films

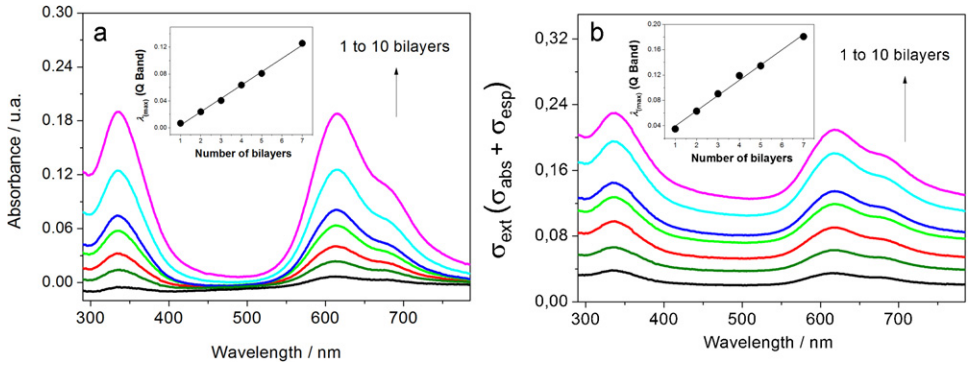

Fig. 2. Growth of LbL films (a) $\{Chit/CoTsPc\}_n$ and (b) $\{Chit\text{-}SWCNTs/CoTsPc\}_n$. Insets: Maximum absorption of the Q band *vs* number of bilayers.

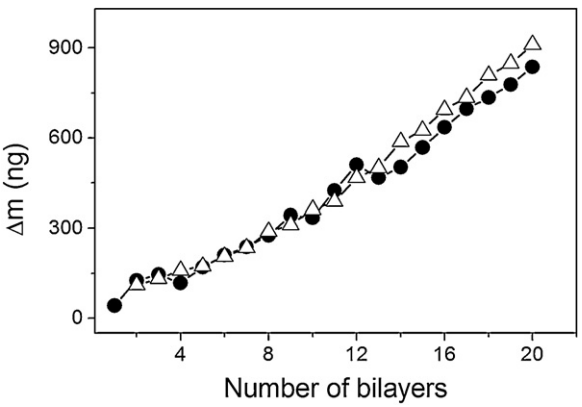

Fig. 3. QCM data for LbL films (Δ) {Chit/CoTsPc} and (●) {Chit-SWCNTs/CoTsPc} up to 20 layers.

containing the nanotubes. Furthermore, both the thickness and the roughness are larger for the SWCNT-containing LbL films. This is consistent with reports for LbL films of PAMAM/NiTsPc and PAMAM-MWCNTs/NiTsPc (PAMAM = poly-amidoamine) [18].

3.3. Electrochemical study from ITO-{Chit/CoTsPc}$_n$ and ITO-{Chit-SWCNTs/CoTsPc}$_n$ modified electrodes

Cyclic voltammetry was employed to investigate the electrochemical properties and growth of Chit/CoTsPc and Chit-SWCNTs/CoTsPc LbL films within the range from −0.8 to 0.8 V (*vs* SCE). We utilized ITO electrodes whose electrochemical properties have been widely studied in nanostructured films [11,13,18]. For LbL films made with CoTsPc and PAH [13], the modified electrodes containing Chit, Chi-SWCNTs and CoTsPc also exhibited better electrochemical response in phosphate buffer solution at pH 6.8. Fig. 5 shows cyclic voltammograms for Chit/CoTsPc (a) and Chit-SWCNTs/CoTsPc (b) with various numbers of bilayers deposited

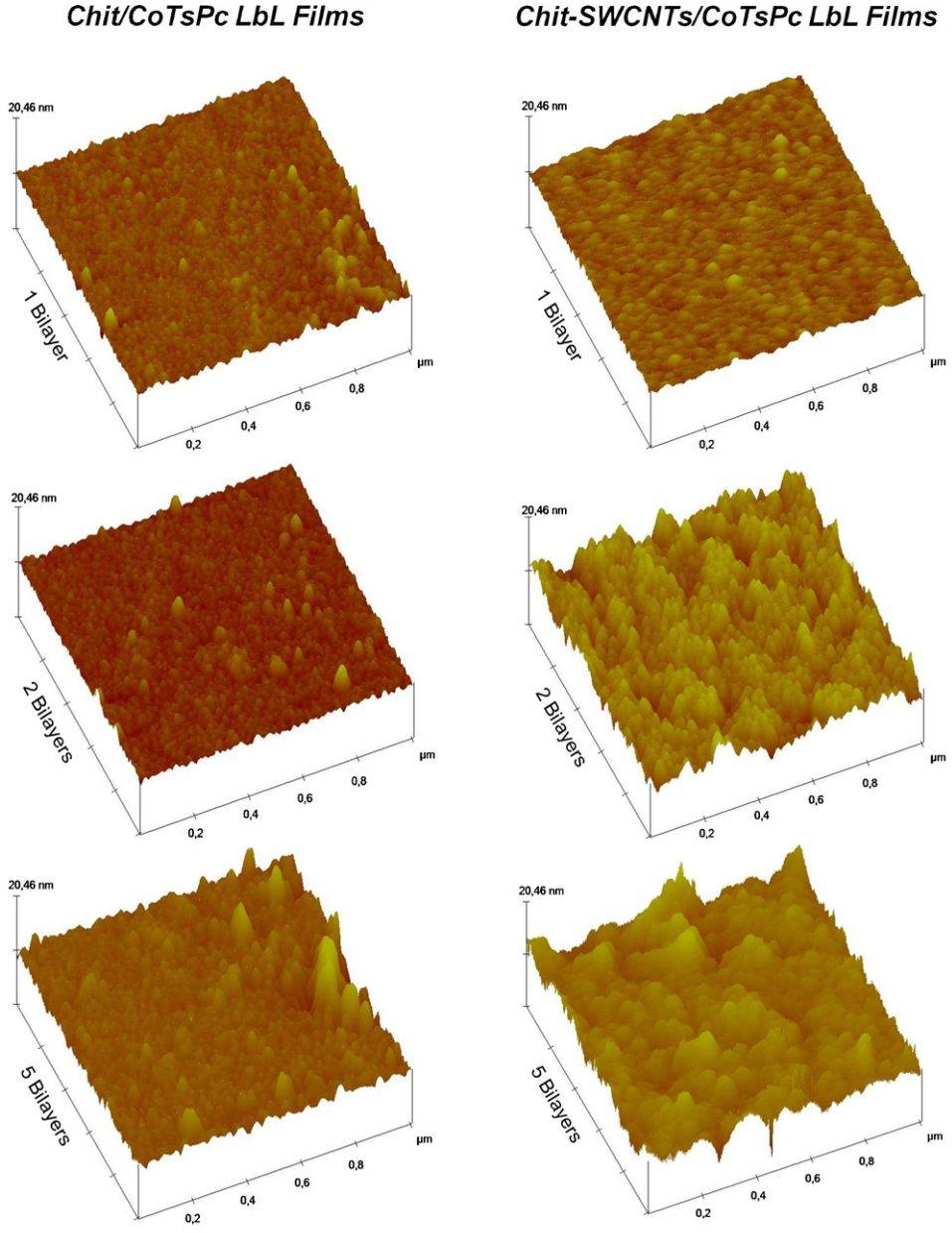

Fig. 4. AFM images for LbL films with 1, 2 and 5 bilayers of {Chit/CoTsPc} and {Chit-SWNT/CoTsPc}.

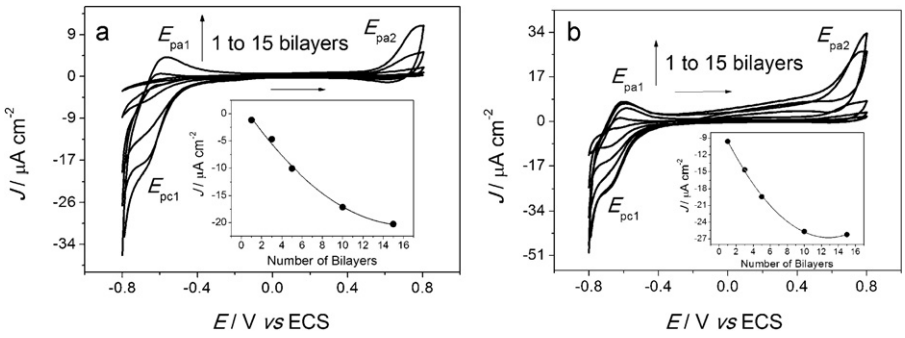

Fig. 5. Cyclic voltammograms for: (a) {Chit/CoTsPc} and (b) {Chit-SWCNTs/CoTsPc} electrodes with different numbers of bilayers (1, 3, 5, 10 and 15). The inset contains the plot for the current of the cathodic peak *vs* number of bilayers. Scan rate 100 mV s^{-1}, electrolyte: PBS solution 0.1 mol L^{-1} pH 6.8, T = 25 °C.

onto ITO. The typical *j–E* electrochemical responses in the cyclic voltammograms increased with the number of bilayers, suggesting that new multilayers were incorporated to the supramolecular architecture after each deposition step.

Both {Chit/CoTsPc} and {Chit-SWNT/CoTsPc} systems exhibited a quasi-reversible one electron process with $E_{1/2} = -0.65$ V attributed to the $[CoTsPc(I)]^{5-}/[CoTsPc(II)]^{4-}$ couple and a peak at 0.80 V associated with the irreversible oxidation process from CoTsPc(II) to CoTsPc(III). One should mention that Chit-SWCNTs/PSS and Chit/PSS LbL films (PSS = poly-styrene sodium sulfate) displayed no electroactivity in the potential range studied. The increasing current in the quasi redox peak at low potential confirms that the electrochemical response from the LbL films is due to the CoTsPc species [11,13]. For the $\{Chit/CoTsPc\}_n$ and $\{Chit\text{-}SWCNTs/CoTsPc\}_n$ films, the anodic (E_{pa1}) and cathodic (E_{pc1}) peaks increased sharply with the number of bilayers, as indicated in the insets of Fig. 5a and b [37]. According to Lundin and co-workers a linear growth is normally observed for strongly charged synthetic polyelectrolytes whereas an exponential-like growth is obtained for weak polyelectrolytes, such as polypeptides or polysaccharides [37]. The latter may be explained by a combination of various phenomena, such as the increase in film surface roughness, complexation of polyelectrolytes above the film surface and interpenetration in adjacent layers [10,18].

In previous studies [11–13] we observed that the number of bilayers affected the electrochemical processes in LbL films containing MTsPc (M = Fe, Ni or Co), especially for LbL films with more than 5 bilayers. Thus, we selected modified electrodes containing 5-bilayers of Chit/CoTsPc and Chit-SWCNTs/CoTsPc to investigate their electrochemical stability. For ITO-$\{Chit\text{-}SWCNTs/CoTsPc\}_5$ modified electrode after 20 cycles in a potential range from −0.8 to 0.8 V, no change on the faradaic currents was observed, even when the same ITO modified electrode was stored in PBS (pH = 6.8) for 1 month. This indicates high electrochemical stability, as confirmed in Fig. S4 in Supplementary Information. However, for the ITO-Chit/CoTsPc modified electrode the electrochemical response was strongly affected after 20 cycles. This latter behavior was not expected for LbL films containing FtTsCo and Chit, for it has been reported that Chit/MTsPc (M = Ni or Fe) [9], PAH/CoTsPc [13] and PAH/NiTsPc films were highly electrochemically stable [12]. In addition, the irreversible (Co^{II}/Co^{III}) conversion in the LbL film containing SWCNTs in Fig. 6 was favored, with an increase in the anodic peak (E_{pa2}) current, indicating the formation of further aggregates on the electrode surface [38]. In particular, the presence of SWCNTs in LbL films led to higher currents than for the films in which Chit was the building block, as shown in Fig. 6. These results may be explained by modulation of the film properties with the supramolecular charge transfer between CoTsPc(II) and SWCNTs, since they should be governed by the dynamic character of the redox reactions, functional recognition, and self-organization [5]. This increase in the faradaic currents is consistent with the AFM images in Fig. 4, where the larger roughness for a 5-bilayer {Chit-SWCNTs/CoTsPc} film may lead to a larger number of active sites with better electrolyte permeability.

The effect of scan rate on the oxidation and reduction currents for 5-bilayer Chit/CoTsPc and Chit-SWCNTs/CoTsPc LbL films was investigated in the 10–500 mV s^{-1} range. Fig. S5 (Supplementary Data) shows a linear relationship between the peak currents and the scan rate for both 5-bilayer films. This indicates strong immobilization and charge transport mechanism in Chit/CoTsPc and Chit-SWCNTs/CoTsPc multilayers, since the SWCNTs are immobilized inside the chitosan matrix [5,10]. Such charge transport has been observed in PAH/MTsPc (M = Fe, Ni or Co) [11–13], Chit/MTsPc (M = Fe or Ni) [9] and PAMAM/NiTsPc or PAMAM-MWCNTs/NiTsPc films [18]. The incorporation of SWCNTs in LbL films containing Chit and CoTsPc improved the electrochemical performance of the CoTsPc species, which may probably be explained by the supramolecular charge transfer between cobalt phthalocyanine and SWCNTs with strong stabilization due to the intimate contact of the adjacent layers [6–11]. Moreover, the CoTsPc species have their redox sites more accessible [11]. The following semi-reactions

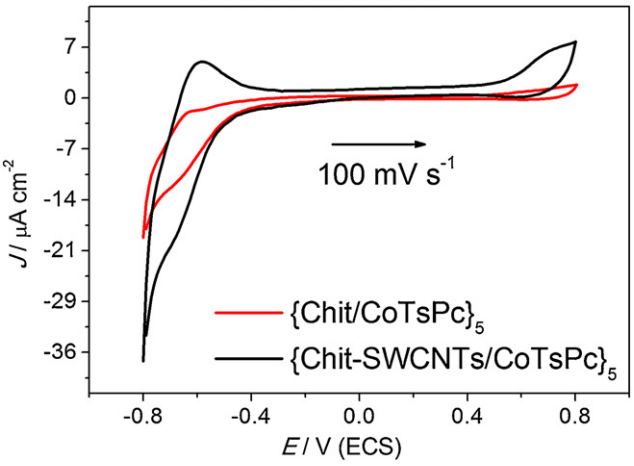

Fig. 6. Cyclic voltammograms of 5-bilayer Chit/CoTsPc and Chit-SWCNTs/CoTsPc LbL films at scan rate of 100 mV s^{-1}. Electrolyte: PBS solution 0.1 mol L^{-1} pH 6.8, T = 25 °C.

describe the electrochemical steps involving charge transport in the LbL films:

$$[Co^{I}TsPc]^{5-} \rightarrow [Co^{II}TsPc]^{4-} + e^{-} \quad (E_{pa1})$$

$$[Co^{II}TsPc]^{4-} \rightarrow [Co^{III}TsPc]^{3-} + e^{-} \quad (E_{pa2})$$

$$[Co^{II}TsPc]^{4-} + e^{-} \rightarrow [Co^{I}TsPc]^{5-} \quad (E_{pc1})$$

Finally, one key advantage of LbL films is the possible control of their properties at the molecular level through functional modulation based on constitutional dynamic chemistry (CDC) without using a specific analyte.

4. Conclusions

The deposition of multilayer {Chit/CoTsPc} and {Chit-SWCNTs/CoTsPc} was successfully obtained, exhibiting a linear growth of the nanoarchitectures with increased thickness and roughness, as revealed by AFM. The incorporation of SWCNTs affects the film morphology and causes an increase in faradaic currents, indicating a possible supramolecular charge transfer interaction between cobalt phthalocyanine and SWCNTs with the CDC effect. The increase in current could in principle be attributed to the larger surface area, but there must be an important contribution from the CDC effect, as indicated by the molecular-level interaction inferred from the FTIR data. The 5-bilayer Chit-SWCNTs/CoTsPc film showed high electrochemical stability in PBS pH 6.8, which did not apply to the 5-bilayer $\{Chit/CoTsPc\}_5$ film. Furthermore, we observed that the number of bilayers affects the charge transport between the redox sites of CoTsPc, since it causes an increase in faradaic currents when an optimized architecture is employed.

The strategy of immobilizing SWCNTs in a chitosan matrix was proven suitable to obtain more stable, electrochemically reversible ITO-{Chit-SWCNTs/CoTsPc} electrodes. It is expected that the film properties will be highly sensitive to the presence of analytes because the CDC effects will be changed. Therefore, the films studied here are promising for developing new sensors and biosensors.

Acknowledgements

The financial support from FAPEPI, CNPq (process number 472369/2008-3 – Universal), and CAPES – Rede Nanobiomed and nBioNet is gratefully acknowledged.

Appendix A. Supplementary data

Supplementary data associated with this article can be found, in the online version, at doi:10.1016/j.matchemphys.2011.08.038.

References

[1] J.M. Lehn, Prog. Polym. Sci. 30 (2005) 814–831.
[2] J.M. Lehn, J.K. Sanders, Supramolecular Chemistry: Concepts and Perspectives, Vch Weinheim, 1995.
[3] J.M. Lehn, Chem. Soc. Rev. 36 (2007) 151–160.
[4] H.E. Toma, J. Braz, Chem. Soc. 14 (2003) 845–869.
[5] W.C. Silva, M. Guix, G.A. Angeles, A. Merkoçi, Phys. Chem. Chem. Phys. 12 (2010) 15505–15511.
[6] G. Decher, Science 277 (1997) 1232–1237.
[7] J. Cho, K. Char, J.D. Hong, K.B. Lee, Adv. Mater. 13 (2001) 1076–1078.
[8] C.H. Porcel, A. Izquierdo, V. Ball, G. Decher, J.C. Voegel, P. Schaaf, Langmuir 21 (2005) 800–802.
[9] F.N. Crespilho, V. Zucolotto, J.R. Siqueira Jr., A.J.F. Carvalho, O.N. Oliveira Jr., F.C. Nart, Int. J. Electrochem. Sci. 1 (2006) 151–159.
[10] J.R. Siqueira Jr., M.H. Abouzar, A. Poghossian, V. Zucolotto, O.N. Oliveira Jr., M.J. Schöning, Biosens. Bioelectron. 25 (2009) 497–501.
[11] W.S. Alencar, F.N. Crespilho, M.V.A. Martins, V. Zucolotto, O.N. Oliveira Jr., W.C. Silva, Phys. Chem. Chem. Phys. 11 (2009) 5086–5091.
[12] W.S. Alencar, F.N. Crespilho, M. Santos, V. Zucolotto, O.N. Oliveira Jr., W.C. Silva, J. Phys. Chem. C 111 (2007) 12817–12821.
[13] A.C. Santos, R.A.S. Luz, L.G.F. Ferreira, J.R. dos Santos Jr., W.C. da Silva, F.N. Crespilho, Quim. Nova 33 (2010) 539–546.
[14] Y. Ofir, B. Samanta, V.M. Rotello, Chem. Soc. Rev. 37 (2008) 1814–1825.
[15] M.N. Zhang, L. Su, L.Q. Mao, Carbon 44 (2006) 276–283.
[16] R.M. Iost, J.M. Madurro, A.G. Brito-Madurro, I.L. Nantes, L. Caseli, F.N. Crespilho, Int. J. Electrochem. Sci. 6 (2011) 2965–2997.
[17] V. Zucolotto, K.R.P. Daghastanli, C.O. Hayasaka, A. Riul Jr., P. Ciancaglini, O.N. Oliveira Jr., Anal. Chem. 79 (2007) 2163–2167.
[18] J.R. Siqueira Jr., L.H.S. Gasparotto, O.N. Oliveira Jr., V. Zucolotto, J. Phys. Chem. C 112 (2008) 9050–9055.
[19] H.H. Yu, T. Cao, L.D. Zhou, E.D. Gu, D.S. Yu, D.S. Jiang, Sens. Actuators B 119 (2006) 512–515.
[20] J.L. Lutkenhaus, P.T. Hammond, Soft Matter 3 (2007) 804–826.
[21] J.F. Quinn, A.P.R. Johnston, G.K. Such, A.N. Zelikin, F. Caruso, Chem. Soc. Rev. 36 (2007) 707–718.
[22] S. Iijima, Nature 354 (1991) 56–58.
[23] E. Katz, I. Willner, ChemPhysChem 5 (2004) 1084–1104.
[24] S.N. Kim, J.F. Rusling, F. Papadimitrakopoulos, Adv. Mater. 19 (2007) 3214–3228.
[25] J.N. Coleman, U. Khan, W.J. Blau, Y.K. Gun'ko, Carbon 44 (2006) 1624–1652.
[26] M.L. Guo, J.H. Chen, J. Li, L.H. Nie, S.Z. Yao, Electroanalysis 16 (2004) 1992–1998.
[27] R.M. Lucente-Schultz, V.C. Moore, A.D. Leonard, B.K. Price, D.V. Kosynkin, M. Lu, R. Partha, J.L. Conyers, J.M. Tour, J. Am. Chem. Soc. 131 (2009) 3934–3941.
[28] D. Lee, T.H. Cui, IEEE Sens. J. 9 (2009) 449–456.
[29] K.Y. Lee, S.H. Yuk, Prog. Polym. Sci. 32 (2007) 669–697.
[30] R. Wang, B. Xia, B.J. Li, S.L. Peng, L.S. Ding, S. Zhang, Int. J. Pharm. 364 (2008) 102–107.
[31] K.L. Purvis, G. Lu, J. Schwartz, S.L. Bernasek, J. Am. Chem. Soc. 122 (2000) 1808–1809.
[32] L. Wang, S.J. Guo, L.J. Huang, S.J. Dong, Electrochem. Commun. 9 (2007) 827–832.
[33] V. Zucolotto, M. Ferreira, M.R. Cordeiro, C.J.L. Constantino, D.T. Balogh, A.R. Zanatta, W.C. Moreira, O.N. Oliveira Jr., J. Phys. Chem. B 107 (2003) 3733–3737.
[34] E.B. Barros, S. Ag Filho, V. Lemos, Carbon 43 (2005) 2495–2500.
[35] J.D. Qiu, H.Z. Peng, R.P. Liang, J. Li, X.H. Xia, Langmuir 23 (2007) 2133–2137.
[36] J. Schmitt, T. Gruenewald, G. Decher, P.S. Pershan, K. Kjaer, M. Loesche, Macromolecules 26 (1993) 7058–7063.
[37] M. Lundin, E. Blomberg, R.D. Tilton, Langmuir 26 (2009) 3242–3251.
[38] J. Chen, A.B.P. Lever, J. Porphyrins Phthalocyanines 11 (2007) 151–159.